Importance of thermal disorder on the properties of alloys: Origin of paramagnetism and structural anomalies in bcc-based $Fe_{1-x}Al_x$

A. V. Smirnov and W. A. Shelton
Computer Science and Mathematical Division, Oak Ridge National Laboratory, Oak Ridge, Tennessee 37831-6367, USA

D. D. Johnson
Materials Science and Engineering and Frederick Seitz Materials Research Laboratory, University of Illinois, Urbana, Illinois 61801, USA

(Received 29 January 2004; published 18 February 2005)

$Fe_{1-x}Al_x$ exhibits interesting magnetic and anomalous structural properties as a function of composition and sample processing conditions arising from thermal or off-stoichiometric chemical disorder, and, although well studied, these properties are not understood. In stoichiometric B2 FeAl, including the effects of partial long-range order, i.e., thermal antisites, we find the experimentally observed paramagnetic response with nonzero local moments, in contrast to past investigations that find either a ferromagnetic or nonmagnetic state, both inconsistent with experiment. Moreover, from this magnetochemical coupling, we are able to determine the origins of the observed lattice constant anomalies found in $Fe_{1-x}Al_x$ for $x \simeq 0.25-0.5$ under various processing conditions.

DOI: 10.1103/PhysRevB.71.064408 PACS number(s): 75.20.En, 81.30.Bx, 75.50.Bb, 61.66.Dk

I. INTRODUCTION

Although bcc-based iron-aluminum ($Fe_{1-x}Al_x$) alloys have been investigated extensively over the years, the complex structural and magnetic properties as a function of composition and type of chemical ordering (in particular, disordered, partially or fully ordered) are not well understood. In fact, while most experimental investigations observe Curie-Weiss-like paramagnetic (PM) response with small ($\sim 0.3\mu_B$) effective moments on Fe,[1–4] electronic-structure calculations for perfectly ordered B2 (β-CuZn) phase obtain a ferromagnetic (FM) state with $\mu \sim 0.7\mu_B$.[4–9] In addition, lattice constant anomalies are observed experimentally in iron-rich Fe-Al, and these anomalies are different depending on whether the samples were quenched, annealed, and/or cold-worked.[10] The processing route used to prepare Fe-Al samples (stoichiometric or not) has key importance because it produces lattice defects that can have a significant effect on the mechanical, structural and magnetic properties of Fe-Al as well as on the intermetallics as a whole. Furthermore, there are competing structures: at 28% (38%) Al at 825 K (475 K), for example, the B2 phase undergoes a second-order transition to $D0_3$ phase. And, due to kinetic limitations, the phase diagram is known only for temperatures $T \geqslant 475$ K. To be able to compare to experiment and to gain an understanding of the anomalies found in this system will require a first-principles method capable of including disorder and temperature effects on equal footing with the electronic structure.

Here, using first-principles methods, we investigate the structural and magnetic properties of bcc-based Fe-Al, including the A2 (bcc disordered), B2, and $D0_3$ phases, as a function of compositionally and thermally induced disorder (antisites). In B2 FeAl, we predict that the PM state competes with the FM state when the state of *partial* long-range order is taken into account. In particular, at $T=0$ K, the PM and FM states are nearly degenerate (<0.25 mRy/atom) over a range of partial long-range order from 50–90 % and is *degenerate* in energy at $\sim$70%. Whereas, the FM state is ~ 0.5 mRy/atom lower than the PM [and nonmagnetic (NM)] state for perfectly ordered B2, in agreement with past theoretical work. More generally, this magneto-chemical coupling leads to anomalies in the average lattice constant in $Fe_{1-x}Al_x$ for $x \simeq 0.25-0.5$ at. % Al, reproducing what has been observed for annealed, quenched and cold-worked samples, which has remained unexplained for one-half of a century. Our results provide a simple and physically reasonable understanding of the, heretofore, anomalous properties found in bcc-based Fe-Al.

II. DISCUSSION

Ordered intermetallics constitute an important class of high-temperature structural materials. One of the most common crystals structures in the intermetallics is the B2 configuration, which, because of its simple atomic arrangement, makes it an ideal model for studying a variety of physical phenomena found in these systems.[11] The physical properties of Fe-Al are quite sensitive to extrinsic defects[12,13] and thermomechanical history.[10,14–16] In fact, B2 FeAl is not fully ordered due to various lattice defects, such as vacancies and antisites, which are thought to play a major role in the mechanical and magnetic behavior of this system. However, the precise concentration of the different lattice defects is not well known. Furthermore, unlike the strongly ordered intermetallics such as B2 NiAl, which forms triple defect structures consisting of two vacancies on the transition metal sublattice and an antisite defect on the Al sublattice, the possible defect structures for the less strongly ordered B2 FeAl are much more complicated, as the formation of both vacancies and antisite defects on the Fe site are thermodynamically stable.[17].

As mentioned, electronic-structure calculations based on the local density approximation (LDA) to density functional theory (DFT)[18] on ideal B2-FeAl obtain a FM state with $\mu \sim 0.7\mu_B$,[4–7,9] in contradiction to the Curie-Weiss-like PM response found in experiment. Calculations based on the disordered local moment (DLM) theory for the paramagnetic state have been performed before, but this approach by itself was unable to explain the observed PM state.[8] Calculations using the generalized gradient approximation (GGA) to DFT, which are known to improve the magnetic ground-state description of elemental bcc Fe,[19] have been employed but do not yield FM $D0_3$-Fe_3Al as a ground state.[20] On the other hand, recent investigations[21,22] have obtained a NM ground state for ideal B2-FeAl within LDA+U procedure, which is an extension of LDA that introduces correlation corrections due to the orbital dependence of the Coulomb interaction. The LDA+U finds a NM ground state for B2-FeAl for a particular range of the empirically chosen parameter U. However, because experiment finds a PM state with *finite* moments, neither ferromagnetic-LDA nor nonmagnetic-LDA+U results explain (or can be confirmed by) existing experimental data. Thus B2-FeAl is either sensitive to the state of order which yields the observed PM state and the LDA+U B2 ground-state is correct but *not relevant* to experiment, or the LDA+U B2 ground state is *wrong* and ferromagnetism would be observed in ideal B2-FeAl. In addition, none of these investigations address any other experimental observation, such as, the composition-dependent structural anomalies found in the system, which are also strongly dependent on the processing route used in synthesizing the material.

In alloys, both short-range order and partial long-range order (LRO), and associated magnetism, are strongly affected by the processing (annealing, quenching, cold-working), which can (and will in the system considered) "freeze in" chemical disorder at some finite temperature (e.g., $0 < T_{\text{Curie}} < T_{\text{processing}} < T_{\text{order-disorder}}$. For example, $D0_3$-Fe_3Al crystal structure has ~8% site disorder according to Bradley and Jay,[23] which was later confirmed separately by Taylor and Cahn.[24,25] Thus, the overall processing procedure affects greatly the materials properties and, therefore, the characterization data obtained from samples that are not completely ordered (due to kinetic limitations). The aforementioned DFT calculations provide results for perfectly ordered states or off-stoichiometric disorder corresponding to $T=0$ K, which may not be directly related to the experimentally assessed data. In fact, Johnson *et al.*[26] have shown that including the thermally induced partial LRO effects allows quantitative comparisons to characterization experiments. In addition, partial disorder can affect the magnetic properties as was demonstrated in the $(Ga_{1-x}Mn_x)As$ (Ref. 27) and $L1_0$ FePt (Ref. 28) systems.

Clearly an investigation of the effects of partial order (both off-stoichiometric and temperature-influenced) on the magnetic and structural properties in the Fe-Al system is in order.

III. COMPUTATIONAL DETAILS

For our electronic-structure calculations, we use the Green's function based, multiple-scattering approach of Korringa, Kohn, and Rostoker (KKR).[29,30] To treat the effects of electron exchange and correlation the local density approximation parameterized by von Barth and Hedin was employed.[31] Furthermore, all calculations are performed using the atomic sphere approximation (ASA) with equal size Fe and Al atomic spheres, see Ref. 32 for more details. For completeness, we note that the ASA energy differences often compare very well to those from full-potential calculations, especially for close-packed metallic systems, see, for example, Refs. 4, 28, and 33.

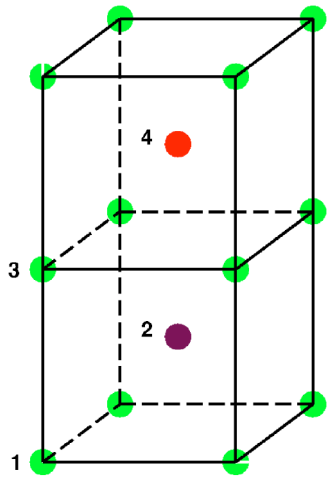

FIG. 1. (Color online) The four-atom cell used to study cubic $D0_3$. For basis atoms 1–4, the translational vectors in lattice units of $T_1=(101)$, $T_2=(011)$, $T_3=(001)$ generate the standard 16-atom (cubic) $D0_3$ cell. In ideal $D0_3$-Fe_3Al, Fe (Al) occupies sites 1–3 (site 4); whereas in B2-FeAl, Fe (Al) atoms occupy odd (even) numbered site. Sites 1 and 3 are always equivalent.

By using the KKR method, we can include chemical and magnetic disorder in the electronic structure and energetics via the coherent potential approximation[34,35] (CPA) modified to incorporate improved metallic screening due to charge-correlations arising from the local chemical environment.[36] The KKR-CPA density-functional formalism provides reliable energetics and structural-related parameters, from fully disordered to ordered configurations.

We describe the PM state by the disorder local moment (DLM) approximation.[37–39] In the DLM the site-dependent average effect of magnetic orientational disorder is self-consistently included, but magnetic short-range order is ignored. It should be noted that the type of chemical ordering (disordered, partially or fully ordered) of the system is not directly dependent on the magnetic state. Thus, our implementation of the KKR-CPA is capable of treating simultaneously chemical disorder, site defects and magnetic (orientational) disorder all on equal footing with the electronic structure (e.g., Slater-Pauling curve[40] or Invar effects.[41,42]).

For all calculations we use a four-atom unit cell (see Fig. 1) based on an underlying bcc crystal lattice that inherently contains the $D0_3$, B2, and A2 (bcc disordered) structures as a function of long-range order (or composition) because each sublattice is composed locally of $Fe_{1-x}Al_x$. Using Fig. 1 it is easy to define the order parameters for our simulations. For example, referenced to the Al sublattice (i=Al), the B2 or-

dering at $x=1/2$ can be defined in terms of a temperature-dependent LRO parameter $\eta(T)$: $c^{\mathrm{Al}}_{i=\mathrm{Al}}=\frac{1}{2}[1+\eta(T)]$ and $c^{\mathrm{Fe}}_{i=\mathrm{Al}}=\frac{1}{2}[1-\eta(T)]$, giving the fully disordered A2 (ordered B2) lattice for $\eta=0$ (1). This describes a static compositional modulation of the A2 phase by a wave vector $\mathbf{k}_0=2\pi(1,1,1)/a$ to yield the partially ordered B2-FeAl ("pseudo-FeAl"), see, e.g., Ref. 43.

Characterization is performed on samples at finite temperatures with $0<\eta(T)<1$. The temperature dependence of $\eta(T)$ can only be obtained from a thermodynamic calculation or measurement. In B2-FeAl at $x=0.5$, $\eta(T)$ varies continuously in the solid phase. Hence, a Landau expansion of the free-energy difference in terms of $\Delta F[\eta(T)]$ (relative to $\eta=0$ state) for a given fixed-sized unit cell (as in Fig. 1) is written as

$$\Delta F^{\sigma}(\eta)=F^{(2),\sigma}(0)\eta^2+O(\eta^4)=E^{\sigma}(\eta)-E^{\sigma}(0)-T\Delta S^{\sigma}(\eta), \tag{1}$$

where odd powers of η are zero due to the translational symmetry of the A2 ($\eta=0$) phase, and ΔS^{σ} is the entropy difference of the system in the magnetic state $\sigma=$(DLM, FM, or NM). We note that the largest contribution to the entropy is the point entropy and this cancels exactly within a common unit cell. Also, when the nearest-neighbor chemical environments are the same (as is the case here), the nearest-neighbor pair entropy cancels exactly. Therefore, the temperature effects are primarily due to antisite disorder, and for a fixed composition, it can be accounted for by analyzing the total energy differences.[26]

In addition to calculations of fully ordered FeAl and Fe_3Al and of B2-FeAl versus η, we also consider $Fe_{1-x}Al_x$ with Al concentration between 25% and 50% which includes fully disordered and off-stoichiometric-disordered B2 and $D0_3$ with and without chemical disorder on the Al sublattices (marked 2 and 4 in Fig. 1). Specifically, the following cases of constituent concentrations are investigated:

(i) for $0.25\leqslant x\leqslant 0.50$, $c^{\mathrm{Al}}_1=c^{\mathrm{Al}}_3=0$, $c^{\mathrm{Al}}_4=1$, $c^{\mathrm{Al}}_2=4x-1$;

(ii) for $0.25\leqslant x\leqslant 0.50$, $c^{\mathrm{Al}}_1=c^{\mathrm{Al}}_3=0$, $c^{\mathrm{Al}}_2=c^{\mathrm{Al}}_4=2x$;

(iii) for $0.25\leqslant x\leqslant 0.25+x_0/2$, $c^{\mathrm{Al}}_4=1-x_0$, $c^{\mathrm{Al}}_1=c^{\mathrm{Al}}_2=c^{\mathrm{Al}}_3=[4x-(1-x_0)]/3$;

(iv) for $0.25+x_0/2\leqslant x\leqslant 0.40$, $c^{\mathrm{Al}}_4=1-x_0$, $c^{\mathrm{Al}}_1=c^{\mathrm{Al}}_3=x_0$, $c^{\mathrm{Al}}_2=(4x-1-x_0)$;

(v) for $0.25\leqslant x\leqslant 0.25+x_0/2$, $c^{\mathrm{Al}}_1=c^{\mathrm{Al}}_3=[4x-(1-x_0)]/3$, $c^{\mathrm{Al}}_2=c^{\mathrm{Al}}_4=0.5-x_0/3$;

(vi) for $0.25+x_0/2\leqslant x\leqslant 0.50$, $c^{\mathrm{Al}}_1=c^{\mathrm{Al}}_3=x_0$, $c^{\mathrm{Al}}_2=c^{\mathrm{Al}}_4=2x-x_0$.

Cases (i) and (ii) have no disorder on sublattices 1 and 3, but have *homogeneous* disorder on Al sublattice 2 for off-stoichiometric $D0_3$ and on Al sublattice 2 and 4 for B2-$Fe_{1-x}Al_x$. Cases (iii)–(vi) reflect structural ordering with partial thermodynamic chemical disorder. That is, the sequence (iii)–(iv)–(vi) imitates a possible transformation from $D0_3$-Fe_3Al to B2-FeAl, whereas (v)–(vi) is for partially ordered B2-FeAl. Concentrations of the constituents for sublattices 1 and 3 are assumed to be the same in both $D0_3$ and B2 with an Al content that is not more than x_0 (see Fig. 1). For illustrative purpose, the value of $x_0=0.09$ is chosen somewhat arbitrarily, although it is comparable with the disorder (the Fe-content on Al-rich sites) reported experimentally for $D0_3$-type FeAl in Ref. 23; for B2-FeAl the case (vi) results in $\eta=1-2x_0=0.82$ which, as it is shown below, is compatible with a range for η of thermodynamically stable partial order for equiatomic FeAl.

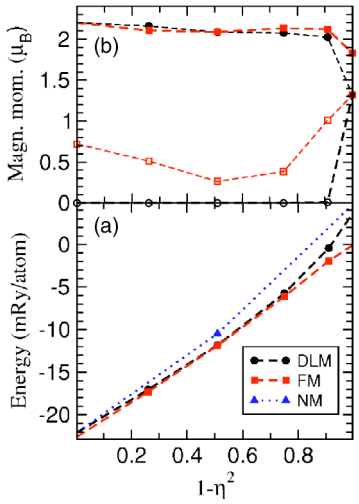

FIG. 2. (Color online) The DLM (circles), FM (squares), and NM (triangles) (a) total energies relative to the A2 FM (mRy/atom) and (b) Fe magnetic moments (μ_B) versus partial order $1-\eta^2$, with filled symbols the Al-rich sites (i.e., the Fe antisites).

IV. PARAMAGNETISM IN B2 FEAL

As mentioned, experimentally B2-FeAl is found to be paramagnetic, with finite local moments. Yet, in agreement with previous theoretical work[4–7,9] our calculations find that the *ideal* B2-FeAl is ferromagnetic. At the theoretical equilibrium lattice parameter $a=5.34$ Bohr, we obtain a magnetic moment of $\approx 0.72\mu_B$ for Fe and $-0.03\mu_B$ for Al, again consistent with the published data (see, for instance, Ref. 4 and references therein). However, such calculations ignore the fact that B2-FeAl is not fully ordered at any finite temperature. Therefore, in Fig. 2, we show the stability of FM, NM, and DLM partially ordered phases of FeAl alloy versus η^2 (long-range order parameter squared) relative to that of the fully disordered FM state, see Eq. (1).

The NM-FM energy difference as a function of η^2 decreases monotonically as $\eta\rightarrow 1$ (increasing order) from 4.8 mRy/atom in the A2 state to 0.5 mRy/atom in the fully ordered B2 structure (in agreement with other $\eta=1$ results, see Introduction). For $\eta=0$ (A2) the DLM-FM energy difference, $\Delta E^{\mathrm{DLM\text{-}FM}}$, is ~ 3.8 mRy/atom ($a^{\mathrm{FM}}=5.45$ Bohr) with $\mu^{\mathrm{FM}}_{\mathrm{Fe}}=1.83\mu_B$ and $\mu^{\mathrm{DLM}}_{\mathrm{Fe}}=1.32\mu_B$, respectively.

Except at $\eta\sim 0.7$ (i.e., 70% LRO with $1-\eta^2=0.5$) where the FM state is degenerate with the DLM state, we find that the FM state is nominally always the lowest energy state for any value of η, $\Delta E^{\mathrm{DLM\text{-}FM}}\leqslant 0.25$ mRy/atom, which is less than thermal energies, for $0.9\geqslant\eta\geqslant 0.5$. For the partially ordered B2 structure $\eta=0.7$ corresponds to a 15% concentration of Al on the Fe rich sublattice, compatible with $\sim 19\%$ found from experiment.[4,10] Both the FM and DLM states have nearly the same lattice parameter (5.36 Bohr). From

Fig. 2 it can be seen that the local Fe antisites moments are finite for any partial long-range order. Whereas Fe atoms on Al-rich sites have nearly the same magnetic moment ($\sim 2.1\mu_B$) for both the FM and the DLM states, the Fe moments for the other sites only exist in the FM state where they are relatively small. The average PM local moments are comparable to the experimentally observed Curie-Weiss moments[4] ($\sim 0.3\mu_B$) at $\eta=0.7$.

It is clear that antisite defects play a crucial role in determining the magnetic configuration. However, in the DLM state at $\eta<0.3$ [see Fig. 2(b)], the Fe magnetic moments exist in both high- and low-spin states. We point out that the electronic origin that gives rise to two different magnetic solutions is similar to other transition metals and alloys.[44,45] In fully ordered ($\eta=1$) B2, the DLM state is equivalent to the NM state, where all local moments are equal to zero; that is, the moments are quenched as there is no antidisorder to sustain the moments.

The key point is that the FM and DLM states can be degenerate or nearly degenerate in the partially ordered (finite η) equiatomic FeAl state. The important quantity in understanding nonzero temperature phenomena is the free energy, and the entropic contributions to the free energy can be accounted for in our calculations within the assumed approximation. While the partially ordered B2-FM phase has no magnetic entropy contribution, the partially ordered B2-DLM paramagnetic state has a large magnetic entropy over a wide range of $\eta(T)$ and temperature. For instance, for a processing temperature of 1300 K (as in Ref. 4) and $\eta=0.7$, $-T\Delta S$ is about 3 mRy in the CPA-DLM model (see Ref. 46 for the DLM probability distribution function) and about 0.9 mRy in the two-state Ising DLM model. Both estimates are well above the respective $\Delta E^{\text{DLM-FM}}$. Thus, partial long range chemical order is stable, making the paramagnetic DLM state the stable configuration at finite temperature, even with only a small degree of disorder.

We note that the theoretical DLM lattice constant is about 3% below the experimental value (≈ 5.50 Bohr). However, such a deviation is comparable with ferromagnetic bcc-Fe, as found in other calculations with the same parametrization of the exchange-correlation functional (see, for instance, Ref. 47). The calculated DLM magnetic moment on an antisite Fe atom (i.e., on Al-rich sites) is close to the value of $2.2\mu_B$ observed by Parthasarathi and Beck[2] for samples quenched in cold water. In addition, Bogner *et al.*[4] have extracted a moment of $\approx 3.43\mu_B$ from Langevin-type behavior of magnetization-field dependence. Bogner *et al.* hypothesized that such a moment could result from a cluster formed by nine nearest-neighbor Fe atoms, which would correspond to a partially ordered alloy with a concentration of Fe atoms on Al sites of 18%, close to the 19% found in their experiment. Such an estimate of Fe-content on Al-rich sites is again consistent with the ~15% determined from our calculation where the FM and DLM are in the partially order state, i.e., the solution with $\eta=1-2(0.15)=0.7$ giving $1-\eta^2=0.51$ on the plots.

V. STRUCTURAL ANOMALIES IN Fe-RICH Fe-Al

Lattice constant anomalies have been experimentally observed in the Fe-rich region of the Fe-Al phase diagram. The lattice constant dependence on concentration is strongly dependent on the quenching or annealing procedure[10] used in synthesizing the material (dashed line in Fig. 3), i.e., thermal antisites and vacancies. For low Al concentration the lattice constant has a nearly linear dependence on concentration. However, between 25%–40% the lattice parameter exhibits nonmonotonic behavior with a maximum lattice constant at $x<0.3$ (for deformed samples at $x\sim 0.34$) and a minimum between $0.34<x<0.43$ with increasing Al content. The exact behavior strongly depends on the type of quenching procedure used during processing.[10] However, the experimental data do not provide quantitative information on sample-dependent (chemical and magnetic) disorder in the observed[23] partially ordered $D0_3$ and B2 structures, which have chemical disorder on each independent sublattice in the partially order structures. It is assumed that the formation of the "pseudo-FeAl" type of ordering is associated with the structural anomalies.[10] To address the anomalies, we consider the "ideal" $D0_3$, case (i) with disorder only on the Al sublattice 4; and ideal B2, case (ii) with disorder on the Al sublattices 2 and 4.

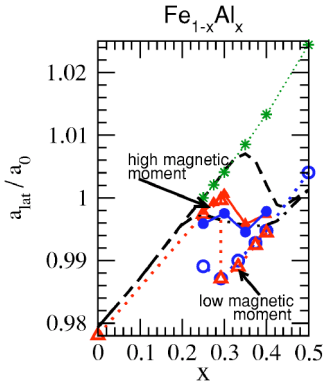

FIG. 3. (Color online) Reduced lattice parameter of $Fe_{1-x}Al_x$ versus x. Theory results are for *off-stoichiometric* $D0_3$ (triangles) and B2 (circles), or the A2 phases (stars). Theoretical a_0 (5.320 Bohr) is the lattice constant of the A2 at $x=0.25$. Filled symbols (triangles/circles) are for $D0_3$/B2 with additional thermal (antisite) disorder, see text. Experimental data is the dashed (dashed-dotted) line for as-deformed samples (quenched from 1273 K) (Ref. 10), and a_0 is that observed lattice constant at $x=0.25$ for deformed sample. Quenching from 523 K yields similar results to high-T quench data.

The results of our $D0_3$ calculations exhibit linear growth of the lattice constant with increasing concentration up to $x\sim 0.29$, while the average magnetic moment (per atom) μ decreases from $1.42\mu_B$ at $x=0.25$ to $1.23\mu_B$. At $x\simeq 0.29$ two degenerate solutions exist for the FM state. The *low-spin* solution has both a smaller $\mu\sim 0.54\mu_B$ and a smaller lattice constant (see Fig. 3). However, the largest discrepancy is for the Fe magnetic moments on sites 1 and 3 where the *low-spin* solution has a significantly smaller magnetic moment on these sites ($\sim 0.2\mu_B$) as compared to the *high-spin* solution ($\sim 1.52\mu_B$) on the same sites. Above $x=0.29$, the *low-spin* solution is energetically more favorable; at elevated temperatures a smoothed transition from high- to low-spin solution with increasing x should be expected since the coexistence of

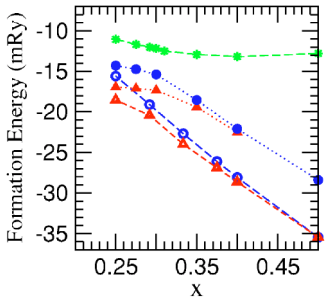

FIG. 4. (Color online) Formation energy of ferromagnetic A2, $D0_3$, and B2 $Fe_{1-x}Al_x$ versus concentration of Al; symbols are chosen as in Fig. 3.

both solutions for a range of Al concentration is possible.

In addition we note that the calculated lattice parameter of the fully disordered A2 phase is almost linear for concentrations of Al up to 34% which agrees well with experimental observations for deformed samples quenched at high temperatures, see Fig. 3. For the A2 phase the energy is about 7 mRy larger than "ideal" $D0_3$ at $x=0.25$, see Fig. 4. The respective energy difference begins to grow rapidly with increasing Al concentration at $x\sim0.3$: from 8.4 mRy at $x=0.29$ to 22.6 mRy at $x=0.5$.

Calculations for the "ideal" B2-disordered $Fe_{1-x}Al_x$ reveals that the lattice parameter is practically indistinguishable from the *low-spin* solution in $D0_3$; however, its magnetic moments are slightly higher than those found in $D0_3$. The difference in the total energy between *pseudo*-FeAl and "ideal" $D0_3$ decreases rapidly (see Fig. 4) from 2.9 mRy/atom at $x=0.25$ to 0.5 mRy/atom at $x=0.40$ and finally to zero at $x=0.5$, where the chemical structures are equivalent. Taking into account the larger *pseudo*-FeAl configurational entropy contribution to the free energy as compared to the partially ordered $D0_3$ phase at the same composition, one reasonably expects that off-stoichiometric $D0_3$ and B2 phases coexist for some values of x at finite temperature. For high enough Al content $D0_3$ would eventually be replaced by the B2 phase as the ground state where again the actual value for the Al concentration would depend on both the temperature and processing procedure.

To illustrate the importance of the thermodynamical chemical disorder we performed calculations for both $D0_3$ [(iii) and (iv)] and B2 [(v) and (vi)] phases. Figure 3 shows a stronger lattice constant dependence on concentration for B2 than for the "high-spin" $D0_3$ solution (i.e., at $x<0.3$). For larger Al content the influence on B2 and $D0_3$ is comparable. Furthemore, the linear dependence of the formation energy on the Al concentration is virtually unaffected by the chemical disorder (excluding the uniform shift), see Fig. 4, for $x>0.34$. However, for smaller Al concentrations this is not the case. This is due to the dependence of the sublattice composition on Al content in (iii)–(vi). The additional effect of partial order on top of off-stoichiometric disorder leads to a plateau in the formation energy, especially for $D0_3$ (see Fig. 4). This is compatible with the shift off stoichiometry for the maximum in the B2-$D0_3$ transition temperature.

Generally, the magnetochemical coupling effect is an ubiquitous phenomenon observed in many materials. It has been used to explain quantitatively, e.g., ordering characterization data[26] and the Invar lattice anomaly in Fe-Ni.[48]

VI. SUMMARY

The structural and magnetic anomalies observed in bcc-based Fe-Al have remained unexplained experimentally and theoretically for over 50 years. As characterization data and their interpretation depend upon the sample preparation and processing, the analysis of their properties based on simulation require the inclusion of these important thermal effects. We have presented a theoretical study that incorporates magnetic, off-stoichiometric, and thermodynamic chemical disorder on equal footing with the electronic structure, exemplifying a quantitative means for studying materials processed at high temperatures where point defects, in particular, antisites, play an important role in determining their properties. We find that partial long-range order due to thermal antisite disorder yields paramagnetic B2 FeAl with finite moments that is stable with respect to the ferromagnetic state, in contrast to past theory but in agreement with experiment. The calculated antisite disorder (i.e., composition of Fe on Al site) associated with the partial long-range order also agrees with that assessed from experiment. Furthemore, this same magnetochemical coupling produces structural anomalies as a function of Al content, as is observed. Our results provide a clear and simple explanation behind the observed paramagnetism and structural anomalies in FeAl. We expect that this type of long-range order effect is responsible for the observed Fe_3Al lattice constant dependence on annealing temperature,[49] as well as the paramagnetism (or spin-glass behavior[50]) in B2-$Fe_{1-x}Al_x$, both of which may be investigated using the approach employed here for $Fe_{0.5}Al_{0.5}$.

ACKNOWLEDGMENTS

This research is supported by the Mathematical, Information and Computational Sciences, Office of Advanced Scientific Computing Research, U.S. Department of Energy at Oak Ridge National Laboratory under Contract No. DE-AC05-00OR22725 with UT-Battelle Limited Liability Corporation, and at the Frederick Seitz Materials Research Laboratory at the University of Illinois Urbana Champaign under Contract No. DEFG02-91ER45439.

[1] M. J. Besnus, A. Herr, and A. J. P. Meyer, J. Phys. F: Met. Phys. **5**, 2138 (1975).
[2] A. Parthasarathi and P. A. Beck, Solid State Commun. **18**, 211 (1976).
[3] H. Domke and L. K. Thomas, J. Magn. Magn. Mater. **45**, 305 (1984).
[4] J. Bogner, W. Steiner, M. Reissner, P. Mohn, P. Blaha, K. Schwarz, R. Krachler, H. Ipser, and B. Sepiol, Phys. Rev. B **58**, 14 922 (1998).
[5] A. R. Williams, J. Kübler, and C. D. Gellat, Phys. Rev. B **19**, 6094 (1979).
[6] H. Chacham, E. Galvao da Silva, D. Guenzburger, and D. E. Ellis, Phys. Rev. B **35**, 1602 (1987).
[7] V. Sundararajan, B. R. Sahu, D. G. Kanhere, P. V. Panat, and G. P. Das, J. Phys.: Condens. Matter **7**, 6019 (1995).
[8] S. K. Bose, V. Drchal, J. Kudrnovsky, O. Jepsen, and O. K. Andersen, Phys. Rev. B **55**, 8184 (1997).
[9] N. I. Kulikov, A. V. Postnikov, G. Borstel, and J. Braun, Phys. Rev. B **59**, 6824 (1999).
[10] W. Hume-Rothery, R. E. Smallman, and C. W. Haworth, *The Structure of Metals and Alloys* (The Metals and Metallurgy Trust of the Institute of Metals and Institution of Metallurgists, London, 1969), pp. 172–173.
[11] I. Baker and P. R. Munroe, in *High Temperature Aluminides and Intermetallics*, edited by S. H. Whang, C. Liu, D. Pope, and J. Stiegler (Minerals, Metals, Material Society, Materials Park, OH, 1990), pp. 425–452.
[12] C. T. Liu, E. H. Lee, and C. G. Mckamey, Scr. Metall. **23**, 875 (1989).
[13] S. Takahashi and Y. Umakoshi, J. Phys.: Condens. Matter **3**, 5805 (1991).
[14] P. Nagpal and I. Baker, Metall. Trans. A **21A**, 2281 (1990).
[15] Y. A. Chang, L. M. Pike, C. T. Liu, A. R. Bilbrey, and D. S. Stone, Intermetallics **1**, 107 (1993).
[16] D. Weber, M. Meurtin, D. Paris, A. Fourdeux, and P. Lesbats, J. Phys.: Condens. Matter **7**, 332 (1997).
[17] C. L. Fu, Y. Y. Ye, M. H. Yoo, and K. M. Ho, Phys. Rev. B **48**, 6712 (1993).
[18] *Theory of the Inhomogeneous Gas*, edited by S. Lundqvist and N. H. March (Plenum, New York, 1983).
[19] C. Elsässer, J. Zhu, S. G. Louie, M. Fäahnle, and C. T. Chan, J. Phys.: Condens. Matter **10**, 5081 (1998).
[20] F. Lechermann, F. Welsch, C. Elsässer, C. Ederer, M. Fähnle, J. M. Sanchez, and B. Meyer, Phys. Rev. B **65**, 132104 (2002).
[21] P. Mohn, C. Persson, P. Blaha, K. Schwarz, P. Novak, and H. Eschrig, Phys. Rev. Lett. **87**, 196401 (2001).
[22] A. G. Petukhov, I. I. Mazin, L. Chioncel, and A. I. Lichtenstein, Phys. Rev. B **67**, 153106 (2003).
[23] A. J. Bradley and A. H. Jay, Proc. R. Soc. London **136**, 210 (1932).
[24] A. Taylor and R. M. Jones, Phys. Chem. Solids **6**, 16 (1958).
[25] A. Lawley and R. W. Cahn, Phys. Chem. Solids **20**, 204 (1961).
[26] D. D. Johnson, A. V. Smirnov, J. B. Staunton, F. J. Pinski, and W. A. Shelton, Phys. Rev. B **62**, R11 917 (2000).
[27] P. A. Korzhavyi *et al.*, Phys. Rev. Lett. **88**, 187202 (2002).
[28] G. Brown, B. Kraczek, A. Janotti, T. C. Schulthess, G. M. Stocks, and D. D. Johnson, Phys. Rev. B **68**, 052405 (2003).
[29] J. Korringa, Physica (Utrecht) **13**, 392 (1947).
[30] W. Kohn and N. Rostoker, Phys. Rev. **94**, 1111 (1954).
[31] U. von Barth and L. Hedin, J. Phys. C **5**, 1629 (1972).
[32] All angular momentum expansions include up to $l_{max}=3$; a semicircular contour in complex plane with 18 points is used to integrate the Green's function over energy; at each energy, a Brillouin zone integration is performed by a special *k*-points method with 144 *k*-points. Such choices provides better than 0.1 mRy/atom relative accuracy in total energy.
[33] N. Zarkevich, D. Johnson, and A. Smirnov, Acta Mater. **50**, 2443 (2002).
[34] D. D. Johnson, D. M. Nicholson, F. J. Pinski, B. L. Györffy, and G. M. Stocks, Phys. Rev. Lett. **56**, 2088 (1986).
[35] D. D. Johnson, D. M. Nicholson, F. J. Pinski, B. L. Györffy, and G. M. Stocks, Phys. Rev. B **41**, 9701 (1990).
[36] D. D. Johnson and F. J. Pinski, Phys. Rev. B **48**, 11553 (1993).
[37] H. Hasegawa, J. Phys. Soc. Jpn. **46**, 1504 (1979).
[38] J. Staunton, B. L. Györffy, A. J. Pindor, G. M. Stocks, and H. Winter, J. Phys. F: Met. Phys. **15**, 1387 (1985).
[39] J. Hubbard, Phys. Rev. B **20**, 4584 (1979).
[40] D. D. Johnson, F. J. Pinski, and J. B. Staunton, J. Appl. Phys. **61**, 3715 (1987).
[41] D. D. Johnson, F. J. Pinski, J. B. Staunton, B. L. Györffy, and G. M. Stocks, in *Physical Metallurgy of Controlled Expansion "INVAR-type" Alloys*, edited by K. Russell and D. Smith (Minerals, Metals, Materials Society, Materials Park, OH, 1989), pp. 3–24.
[42] D. D. Johnson and W. A. Shelton, in *The INVAR Effect—A Centennial Symposium*, edited by J. Wittenauer (Minerals, Metals, Materials Society, Materials Park, OH, 1997), p. 6374.
[43] A. G. Khachaturyan, *Theory of Structural Phase Transformations in Solids* (Wiley, New York, 1983), pp. 45 and 46.
[44] V. L. Moruzzi, Phys. Rev. B **41**, 6939 (1990).
[45] V. L. Moruzzi and P. M. Marcus, Phys. Rev. B **45**, 2934 (1992).
[46] J. Staunton, B. L. Gyorffy, G. M. Stocks, and J. Wadsworth, J. Phys. F: Met. Phys. **16**, 1761 (1986).
[47] D. J. Singh, W. E. Pickett, and H. Krakauer, Phys. Rev. B **43**, 11 628 (1991).
[48] V. Crisan, P. Entel, H. Ebert, H. Akai, D. D. Johnson, and J. B. Staunton, Phys. Rev. B **66**, 014416 (2002).
[49] Y. P. Selisskiy, Fiz. Met. Metalloved. **4**, 191 (1957).
[50] P. Shukla and M. Wortis, Phys. Rev. B **21**, 159 (1980).